



A comparative study of the interaction of two structurally analogous ruthenium complexes with human telomeric G-quadruplex DNA

Shuo Shi ^{a,*}, Hai-Liang Huang ^a, Xing Gao ^a, Jun-Liang Yao ^a, Chun-Yan Lv ^a, Juan Zhao ^a, Wen-Liang Sun ^a, Tian-Ming Yao ^{a,*}, Liang-Nian Ji ^{a,b}

^a Department of Chemistry, Tongji University, Shanghai 200092, PR China

^b MOE Laboratory of Bioinorganic and Synthetic Chemistry, School of Chemistry and Chemical Engineering, Sun Yat-Sen University, Guangzhou 510275, PR China

ARTICLE INFO

Article history:

Received 19 August 2012

Received in revised form 19 December 2012

Accepted 20 December 2012

Available online 29 December 2012

Keywords:

Ruthenium complexes

G-quadruplex DNA

Comparative study

Spectral properties

Molecular docking

ABSTRACT

Two new polypyridine ligands and their corresponding ruthenium(II) complexes have been prepared and characterized. The interactions of both complexes with human telomere quadruplex DNA (both the antiparallel basket and the mixed-hybrid G-quadruplex) have been studied by circular dichroism (CD), CD melting, UV-visible (UV-Vis), fluorescent intercalator displacement (FID) assays and molecular docking studies. The results show that both complexes can stabilize G-quadruplexes DNA and two complexes show different binding affinity for different G-quadruplexes DNA. The 1:1 stoichiometry was confirmed in the buffered solutions by the UV-Vis spectrophotometer using Job's plot method and molecular docking studies. We have also investigated the interaction between the complexes and duplex DNA to gain some insight into the selectivity of the complexes for G-quadruplex structures. FID studies have shown that the complexes have a modest selectivity for G-quadruplex versus duplex DNA.

© 2012 Elsevier Inc. All rights reserved.

1. Introduction

G-rich DNA sequences can adopt a special class of DNA structure called a G-quadruplex, which comprises a stack of G-tetrads, the planar association of four guanines in a cyclic Hoogsteen hydrogen bond [1–3]. Recently, bioinformatic studies have shown that in the human genome there are approximately 350,000 guanine-rich sequences that can potentially form G-quadruplex DNA structures [4–6]. G-quadruplexes DNA are highly dynamic and polymorphic DNA structures, and the structures and the stability of the G-quadruplexes depend on monocations [7]. The best-studied example is the human telomeric repeat AG3(T2AG3)3 quadruplex, the NMR structure of AG3(T2AG3)3 in the presence of Na⁺ was an antiparallel basket quadruplex [8], the X-ray structure for the same sequence in the presence of K⁺ revealed a parallel propeller quadruplex [9], whereas, it favored a mixed-hybrid (parallel/antiparallel) structure in the presence of K⁺ solution [10,11]. It has been suggested that these secondary DNA structures could be involved in the regulation of several key biological processes [12,13]. There is now mounting evidence showing that formation of quadruplexes in guanine-rich regions of the genome may play important roles in regulating gene expression. For example, the promoter regions of certain oncogenes such as c-myc and c-kit are guanine rich, and formation of G-quadruplexes in these regions has been proposed to regulate the corresponding oncogene's transcription [14–18]. On

the other hand, formation of G-quadruplex DNA structures in the human telomere has been shown to inhibit telomerase (an enzyme over expressed in approximately 85% of cancer cells and which plays an important role in cancer cell immortalization) [19–22]. These potential roles of G-quadruplex DNA structures have stimulated a search for specific molecules that stabilize G-quadruplexes in either the promoter regions of oncogenes or in the telomeric region. Such molecules could provide a basis for the development of novel anticancer drugs.

Over the past 10 years, a rational approach to design small molecules that can selectively interact with G-quadruplex DNA has emerged. A number of promising small organic molecules have been devised to inhibit telomerase and/or regulate the transcription of certain oncogenes. These molecules range from acridine derivatives, cationic porphyrin derivatives, ethidium derivatives, anthraquinone derivatives, perylene derivatives, and telomestatin and others planar compounds [23–28]. These ligands have the common feature of extended planar aromatic electron-deficient chromophore with cationic substituents. In contrast to the large number of organic molecules reported to bind to this secondary structure of DNA, metal complexes have only recently started to be systematically investigated [29–33]. Metal complexes have clear advantages over their organic counterparts, such as, electropositive, modular and facile synthesis, interesting optical and magnetic properties etc, which offer an ideal platform for sharp drug design and rationalization of structural interactions [29]. These studies have shown the great potential metal complexes have in binding to (and stabilizing) quadruplexes, and in doing so, inhibiting telomerase or regulating gene expression of certain oncogenes.

* Corresponding authors. Tel.: +86 21 6598 3292; fax: +86 21 6598 2287.

E-mail addresses: shishuo@tongji.edu.cn (S. Shi), tmyao@tongji.edu.cn (T.-M. Yao).

Ruthenium complexes that bind noncovalently to duplex DNA have been of great interest for the last 30 years, as this class of molecules has potential as DNA-conformational probes, anticancer drugs, or initiators for electron-transfer studies on duplex DNA [34–38]. Ruthenium complexes containing planar aromatic ligands that bind to DNA have many convenient features, including the ease with which the ligand can be attached to the metal in a controlled manner, strong visible absorbance, due to a localized metal-to-ligand charge transfer (MLCT) and strong fluorescence emission. Just as the unique properties of ruthenium complexes have been successfully used to probe duplex DNA, however, it is important to note that these complexes are only in the beginning stages of development as G-quadruplex DNA binders. We reported previously a novel dinuclear complex $\text{Ru}_2(\text{obip})\text{L}_4$ (obip = 2-(2-pyridyl)imidazo[4,5-f][1,10]-phenanthroline, L = 2,2'-bipyridine) which has the remarkable ability to promote the formation and stabilization of G-quadruplex DNA [31]. Recently, our laboratory found that $[\text{Ru}(\text{L})_2(\text{dppz})]^{2+}$ (L = 2,2'-bipyridine or 1,10-phenanthroline, dppz = dipyrido[3,2-a:2',3'-c]phenazine) can serve as a prominent molecular “light switch” for both G-quadruplexes and i-motif, which prefers binding G-quadruplexes over i-motif [39,40]. Furthermore, we reported the first example of a reversible G-quadruplex DNA light switch, the switch can be cycled through the competition of $[\text{Fe}(\text{CN})_6]^{4-}$ ions and G-quadruplex DNA [41].

Herein, we report the synthesis, characterization and G-quadruplex DNA binding of two new ruthenium(II) complexes (Scheme 1) $[\text{Ru}(\text{phen})_2(\text{bppp})]^{2+}$ (**1**) and $[\text{Ru}(\text{phen})_2(\text{pppp})]^{2+}$ (**2**) (phen = 1,10-phenanthroline, bppp = 12-bromo-pyrido[2',3':5,6]pyrazino[2,3-f][1,10]phenanthroline, pppp = 12-phenylpyrido[2',3':5,6]pyrazino[2,3-f][1,10]phenanthroline). We hope that our results will aid in the understanding

of G-quadruplexes DNA recognition and binding by Ru(II) complexes, as well as laying the foundation for the rational design of new anticancer therapeutic agents.

2. Materials and methods

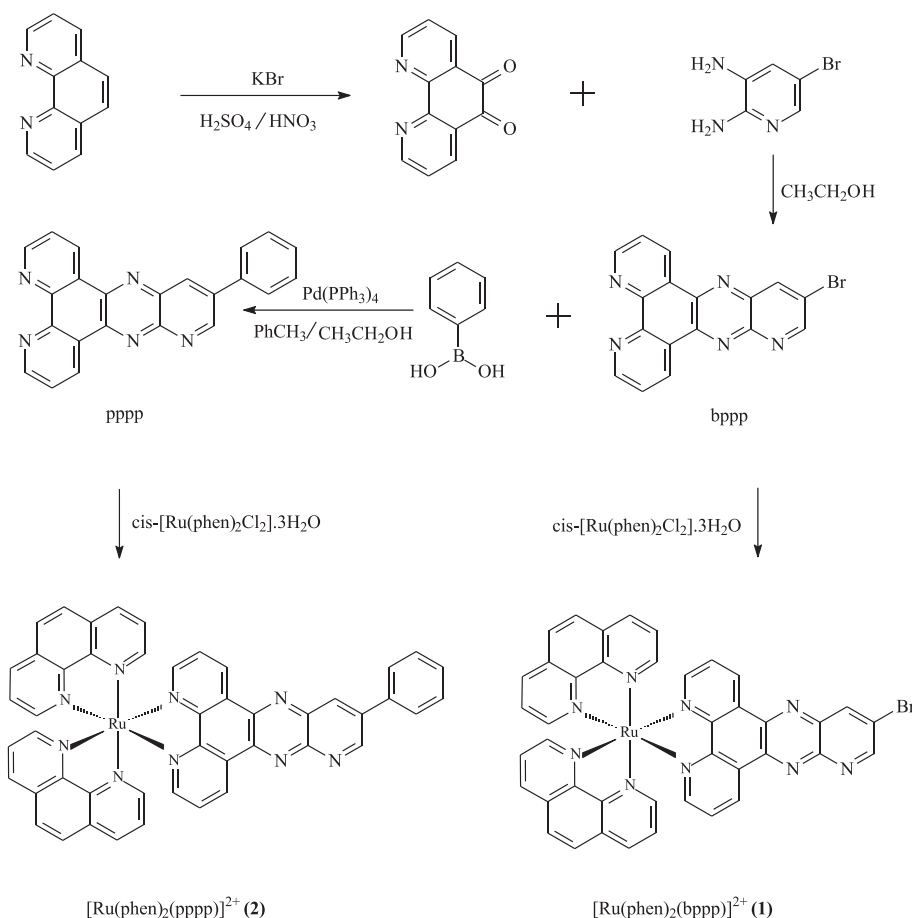
2.1. Materials and chemicals

1,10-phenanthroline-5,6-dione, $\text{cis-Ru}(\text{phen})_2\text{Cl}_2 \cdot 3\text{H}_2\text{O}$ were synthesized according to the literature methods [42]. The other chemicals were obtained from commercial sources and used without further purification unless otherwise noted. DNA oligomers 5'-AGGGTTAGGGTTAGGGTTAGGG-3' (22AG) and 16 base-pair complementary duplex DNA (5'-CCTCGGCCGCCGACC-3') were purchased from Sangon (Shanghai, China) and used without further purification. Concentrations of these oligomers were determined by measuring the absorbance at 260 nm after melting. Single-strand extinction coefficients were calculated from mononucleotide data using a nearest-neighbour approximation [43]. The formation of intramolecular G-quadruplexes was carried out as follows: the oligonucleotide samples, dissolved in different buffers, were heated to 90 °C for 5 min, gently cooled to room temperature, and then incubated at 4 °C overnight. Buffer A: 100 mM KCl, 10 mM Tris, pH 7.0; Buffer B: 100 mM NaCl, 10 mM Tris, pH 7.0.

2.2. Synthesis

2.2.1. bppp (12-bromo-pyrido[2',3':5,6]pyrazino[2,3-f][1,10]phenanthroline)

A mixture of 1,10-phenanthroline-5,6-dione (640 mg, 3.0 mmol) and 2,3-Diamino-5-bromopyridine (560 mg, 3.0 mmol) in 20 mL of



Scheme 1. Synthetic routes for the preparation of the complexes $[\text{Ru}(\text{phen})_2(\text{bppp})]^{2+}$ (**1**) and $[\text{Ru}(\text{phen})_2(\text{pppp})]^{2+}$ (**2**).

methanol was refluxed for 2 h. Upon cooling, the yellow precipitate was collected by filtration and further recrystallized from methanol. Yield: 880 mg, 82%. Anal. Calcd for $C_{17}H_8BrN_5$: C, 56.38; H, 2.23; N, 19.34. Found: C, 56.37; H, 2.24; N, 19.36. FAB-MS: $m/z = 362.0 [M + H]^+$.

2.2.2. *pppp* (12-phenylpyrido[2',3':5,6]pyrazino[2,3-f][1,10]phenanthroline)

A solution of *bppp* (362 mg, 1.0 mmol), phenylboronic acid (134 mg, 1.1 mmol) and potassium carbonate (15 mL, 2 M) in 20 mL of toluene and 10 mL of ethanol was fully degassed and refluxed at 90 °C under argon 3 h. Then tetrakis(triphenylphosphine)palladium(0) ($Pd(PPh_3)_4$) (116 mg, 0.1 mmol) was added and another 12 h of heating, the reaction mixture was cooled to room temperature. The solvents were evaporated, water was added and extracted with chloroform. The organic fractions were collected and evaporated to dryness, giving 251 mg of a yellow solid (70% yield). Anal. Calcd for $C_{23}H_{13}N_5$: C, 76.87; H, 3.65; N, 19.49. Found: C, 76.84; H, 3.64; N, 19.47. FAB-MS: $m/z = 360.4 [M + H]^+$.

2.2.3. $[Ru(phen)_2(bppp)](PF_6)_2$ (**1**)

Cis- $[Ru(phen)_2Cl_2] \cdot 3H_2O$ (170 mg, 0.30 mmol) and *bppp* (109 mg, 0.30 mmol) were added to 20 mL ethylene glycol–water (9:1, v/v). The mixture was refluxed for 6 h under an argon atmosphere. The cooled reaction mixture was diluted with water (50 mL) and filtered to remove solid impurities. And then, to the filtrate was added ammonium hexafluorophosphate. The precipitated complex was dried, dissolved in a small amount of acetonitrile, and purified by chromatography over alumina, using MeCN–toluene (3:1, v/v) as eluent and further recrystallized from acetone/diethyl ether (1:5, v/v). Yield: 280 mg, 84%. 1H NMR [$(CD_3)_2SO$]: δ 9.62 (1H, d), 9.60 (1H, d), 9.54 (1H, d), 9.34 (1H, d), 8.81 (4H, t), 8.42 (4H, s), 8.29 (2H, d), 8.25 (2H, d), 8.07 (2H, d), 7.95 (2H, t), 7.85–7.77 (4H, m). Calc. for $C_{41}H_{24}BrF_{12}N_9P_2Ru$: C, 44.22; H, 2.17; N, 11.32. Found: C, 44.20; H, 2.19; N, 11.38. ESI-MS: m/z 824.0 ($[M-2PF_6 + H]^+$).

2.2.4. $[Ru(phen)_2(pppp)](PF_6)_2$ (**2**)

With 0.30 mmol, 0.108 g *pppp* in place of *bppp*, this complex was obtained by a procedure similar to that described for **1**. Yield: 290 mg, 87%. 1H NMR [$(CD_3)_2SO$]: 9.94(1H, d), 9.67(1H, d), 9.61(1H, d), 9.19 (1H, d), 8.82(4H, t), 8.42 (4H, s), 8.30 (2H, t), 8.25 (2H, d), 8.20 (2H, d), 8.08 (2H, d), 7.96 (2H, t), 7.83 (2H, m), 7.79 (2H, m), 7.68 (2H, t), 7.62 (1H, d). Calc. for $C_{47}H_{29}F_{12}N_9P_2Ru$: C, 50.82; H, 2.63; N, 11.35. Found: C, 50.80; H, 2.63; N, 11.39. ESI-MS: m/z 821.2 ($[M-2PF_6 + H]^+$).

The NMR spectra of $[Ru(phen)_2(bppp)]^{2+}$ (**1**) and $[Ru(phen)_2(pppp)]^{2+}$ (**2**) as well as their definition have been given in the supplementary information (Fig. S1).

2.3. Physical measurements

Elemental analyses (C, H and N) were carried out with a Perkin–Elmer 240C elemental analyzer. 1H NMR spectra were recorded on a Bruker DRX-400 NMR spectrometer with $(CD_3)_2SO$ as solvent and $SiMe_4$ as an internal standard. Electrospray ionisation mass spectra (ESI-MS) were acquired on a Thermo Finnigan LCQ DECA XP ion trap mass spectrometer, equipped with an ESI source.

2.3.1. CD measurements and CD melting profiles

Circular dichroism (CD) spectra were measured on a Jasco J-810 spectropolarimeter. The oligonucleotide samples were dissolved in two different buffered solutions in this study: (a) in K^+ buffer (pH 7.0); (b) in Na^+ buffer, (pH 7.0). The corresponding samples of the DNA (22AG) at a concentration of 5 μM were dissolved in different solutions and placed in a quartz cuvette. During the titration, aliquot (1–10 μL) of $[Ru(phen)_2(L)]^{2+}$ solution was added to the cuvette, and the solutions were mixed by repeated inversion. After the solutions were mixed for ~5 min, the CD spectra were recorded. The

titration processes were repeated until there was almost no change, indicating binding saturation had been achieved. For each sample, at least four spectrum scans were accumulated over the wavelength range of 200–350 nm at the temperature 25 °C in a 1.0 cm path length cell at a scanning rate of 50 nm/min. The instrument was flushed continuously with evaporated liquid nitrogen throughout the experiment. The scan of the buffer alone was subtracted from the average scan for each sample. In the melting studies, the temperature of the sample was maintained by a Julabo HD-25 temperature controller. The melting curves of the G-quadruplex were measured with the intensity at 295 nm. Before the CD spectroscopy, all the samples were thermally treated as described above. The heating rate was 1.0 °C min^{-1} .

2.3.2. Absorption spectra titrations

Absorption spectra titrations were carried out at room temperature to determine the binding affinity between DNA and complex. Initially, 3000 μL solutions of the blank buffer and the ruthenium complex sample (10 μM) were placed in the reference and sample cuvettes (1.0 cm path length), respectively, and then first spectrum was recorded in the range of 200–600 nm. During the titration, aliquot (1–10 μL) of buffered DNA solution was added to each cuvette to eliminate the absorbance of DNA itself, and the solutions were mixed by repeated inversion. After the solutions were mixed for ~5 min, the absorption spectra were recorded. The titration processes were repeated until there was no change in the spectra for four titrations at least, indicating binding saturation had been achieved. The changes in the metal complex concentration due to dilution at the end of each titration were negligible.

2.3.3. Job's plots of UV-visible (UV-Vis) absorption

According to the literature procedure, equimolecular solutions of compounds and G-quadruplex DNA are mixed in various proportions. The mole fraction of each molecular was varied from 0.1 to 1.0, in 0.1 increments, while the total concentration was kept at 10 μM . The difference (ΔA) between each experimental value and that calculated as the sum of the contributions of the two separate components is plotted against the molar fractions. The resulting curves display a break point at the molar fraction corresponding to the stoichiometry of the complex. The absorption of each sample was recorded at room temperature and baseline values were routinely subtracted from the spectra.

2.3.4. Fluorescent intercalator displacement (FID) assay

The 22AG strand 5'-AGGGTTAGGGTTAGGGTTAGGG-3' and 16 base-pair complementary strand 5'-CCTCGGCCGCCGACC-3' were used for the human telomeric G-quadruplex and duplex DNA, respectively. FID experiments were performed as follows: onto a mixture of prefolded DNA (1 μM) and thiazole orange (TO) (2 μM), in 100 mM K^+ buffer or 100 mM Na^+ buffer, an increasing amount of the corresponding molecule under study was added (0.25–20 μM) by a 3 min equilibration period before the fluorescence spectrum is recorded. Emission spectra were measured on a Shimadzu RF-5000 spectrofluorophotometer. The excitation wavelength was 492 nm, and the emission spectrum was collected from 500 to 750 nm. Excitation and emission slits were set at 10 and 10 nm, respectively. The fluorescence of samples was measured at 25 °C. The titration processes were repeated until there was no change in the spectra for at least four titrations indicating binding saturation had been achieved.

2.3.5. Molecular docking studies

Both the antiparallel basket quadruplex (Protein Data Bank (PDB) ID: 143D) and the mixed parallel/antiparallel structure (PDB ID: 2HY9) were used as an initial model to study the interaction between $[Ru(phen)_2(L)]^{2+}$ and 22-mer telomeric G-quadruplex DNA.

$[\text{Ru}(\text{phen})_2(\text{L})]^{2+}$ was optimized using density functional theory (DFT) with a LanL2MB basis set [44]. The optimized structure of the ruthenium complex was used to do the docking. When preparing for docking DNA and complex ($[\text{Ru}(\text{phen})_2(\text{L})]^{2+}$), necessary modifications were carried out: (1) add all hydrogens or just non-polar hydrogens; (2) assign partial atomic charges to the complex and the macromolecule (Gasteiger or Kollman United Atom charges); (3) merge non-polar hydrogens and Set up rotatable bonds in the complex; (4) output PDBQT (Protein Data Bank, Partial Charge (Q), & Atom Type (T)) files from traditional PDB files are also created for the side chain coordinates. Docking was carried out with the AutoDock 4.2 Lamarckian Genetic Algorithm (LGA) [45–47]. For antiparallel basket G-quadruplex structure, to create a pseudo-intercalation complex binding site between the diagonal loop and the G-quartet segment of the structure (at the 5' AG step) in the human intramolecular G-quadruplex NMR structure (PDB code: 143D), the following steps have been employed: (1) two phosphate backbones are broken at the 5' AG step; (2) the two halves of the structure are separated so that the separation of the A:A base pair and the G-quartet is increased from 3.4 to 6.8 Å; (3) the sugar-phosphate backbones are reconnected [48,49]. As for the mixed-hybrid G-quadruplex structure, two adenines from each end of the mixed-hybrid type structure (PDB code: 2HY9) were removed and similar operations to increase the separation between loop base pairs and the G-quartet were performed [50]. In the autodocking, DNA was enclosed in the grid defined by Auto Grid having 0.375 Å spacing and parameters (supplied with the program package) were used for dispersion/repulsion, hydrogen bonding, electrostatics, and desolvation, respectively. Auto Grid performed a precalculated atomic affinity grid maps for each atom type in the complex plus an electrostatics map and a separate desolvation map present in the substrate molecule. Then, during the AutoDock calculation, the energetics of a particular complex configuration is evaluated using the values from the grids. The output from AutoDock was rendered with Accelrys Discovery Studio 3.0 Client [51].

3. Results and discussion

CD spectroscopy was employed to determine the solution formation of G-quadruplex in the absence or presence of synthetic complexes in either K^+ or Na^+ buffers. As shown in Fig. 1(a), the CD spectrum of the human telomeric sequence 22AG in the presence of 100 mM K^+ exhibited a large positive band at 290 nm, a small positive band at 270 nm, and a negative band at 235 nm, which suggested that 22AG might exist as a mixed-hybrid quadruplex DNA containing parallel and antiparallel structure. On the other hand, the CD spectrum of the same sequence in the presence of 100 mM Na^+ ions had a 295 nm positive band and a 265 nm negative band, which was characteristic of an antiparallel G-quartet structure consistent with the results of previous NMR studies [52–55]. Upon addition of either **1** or **2** to 22AG aqueous solution in K^+ buffer (Fig. 1(a)) resulted in significant changes to the CD spectrum, including the observation of an isoelliptical point at 259 nm, which suggested the presence of both free and bound quadruplex DNA in solution. With increasing **1** or **2** binding, the negative band at about 260 nm (characteristic of antiparallel G-quartet structure) started to appear and increased sharply. The emergence of homogeneous antiparallel basket type characteristics with the distinctive minima pattern of 265 nm indicated that both **1** and **2** converted the preformed mixture of G-quadruplexes into the antiparallel basket type G-quadruplex under K^+ conditions. These significant changes in the CD spectrum of 22AG after the addition of **1** or **2** were consistent with both complexes binding to the DNA and thus causing substantial change(s) in the conformation of the DNA. However, upon addition of **1** or **2** to 22AG in buffer containing Na^+ , no obvious spectral changes were observed (Fig 1(c, d)), which implied that the conformation of G-quadruplex was stabilized by Na^+ , and either **1** or **2** could not change the conformation of G-quadruplex at high ionic strength.

The stability of the adducts of the complexes with the G-quadruplex was studied by CD spectroscopy at variable temperature using 22AG incubated with either complex **1** or **2** in the presence of K^+ or Na^+ .

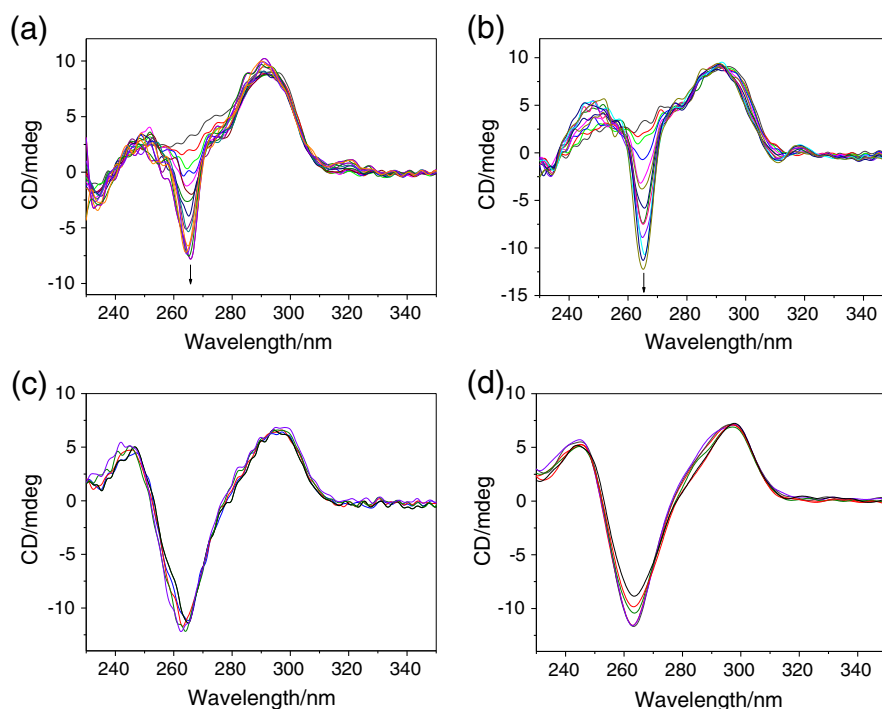


Fig. 1. CD titration of 22AG by adding complex **1** or **2** in K^+ buffer (100 mM KCl, 10 mM Tris, pH 7.0) or Na^+ buffer (100 mM NaCl, 10 mM Tris, pH 7.0) at 25 °C. CD spectra of (a) 22AG + **1** in K^+ buffer; (b) 22AG + **2** in K^+ buffer; (c) 22AG + **1** in Na^+ buffer and (d) 22AG + **2** in Na^+ buffer.

Consistent with previous studies [56,57], 295 nm was chosen to study the influence of the complex on the stability of G-quadruplex DNA. The normalized CD intensity of 22AG with 5 μM complex in different buffers at 295 nm vs the temperature was shown in Fig. 2. The transition temperature of the G-quadruplex increased from 55.3 to 61.3 $^{\circ}\text{C}$ in Na^+ buffer and increased from 65.2 to 71.7 $^{\circ}\text{C}$ in K^+ buffer induced by complex **2**, in which an increase in the melting temperature of the G-quadruplex indicated a stabilizing effect. Under the same conditions, the transition temperature of the G-quadruplex increased from 55.3 to 60.2 $^{\circ}\text{C}$ in Na^+ buffer and increased from 65.2 to 69.8 $^{\circ}\text{C}$ in K^+ buffer induced by complex **1**. These data are indicative of the strong propensity of both complexes to form stable interactions with G-quadruplexes resulting in the formation of bound complexes whose thermal stabilities are markedly enhanced from native G-quadruplexes. As for complex **2**, it had bigger influence on the thermal stability G-quadruplex DNA either in Na^+ buffer or in K^+ buffer (Fig. 2) compared with complex **1**, which implies that a higher affinity of **2** for the human telomeric sequence and resulting in bigger stability of the telomeric G-quadruplex than that of complex **1**. Since the ancillary ligand (phen) of the complexes **1** and **2** is the same, their differential DNA-binding affinities must be attributed to the different main ligands. On going from the main ligand bppp to pppp, the hydrophobicity of the ligand pppp is greater than the ligand bppp and the square π -aromatic surface of pppp is larger than bppp. Both factors are advantageous to the G-quadruplexes DNA-binding. Therefore, synthetically considering these factors, the difference of the G-quadruplexes DNA-binding affinity of complexes **1** and **2** can be well understood.

The application of electronic absorption spectroscopy in DNA-binding studies is one of the most useful techniques. The high-energy band around 262 nm is attributed to the $\pi \rightarrow \pi^*$ transitions corresponding to the phenanthroline moiety of the ligands. The low-energy band at 438 nm for complex **1** is attributed to the overlap of $\text{Ru}(\text{d}\pi) \rightarrow \text{phen}(\pi^*)$ and $\text{Ru}(\text{d}\pi) \rightarrow \text{bppp}(\pi^*)$. Apart from these, absorption bands centered at 376 and 392 nm for complexes **1** and **2** can be assigned to the intraligand (IL) $\pi \rightarrow \pi^*$ transition of bppp and pppp, respectively, by comparison with the spectrum of other polypyridyl Ru(II) complexes [58–60].

Absorption spectra titrations were performed to determine the binding affinity of complex to 22AG too. DNA sample was added in aliquots sequentially to complex solutions, with absorbance spectra recorded after each addition. The changes in the spectral profiles during titration were shown in Fig. 3. When 22AG is added into complex **2** solutions, notable red shift and hypochromism are observed. Furthermore, bigger hypochromism is observed for complexes upon addition of the mixed-hybrid quadruplex DNA than the antiparallel basket quadruplex DNA under the same conditions. For example,

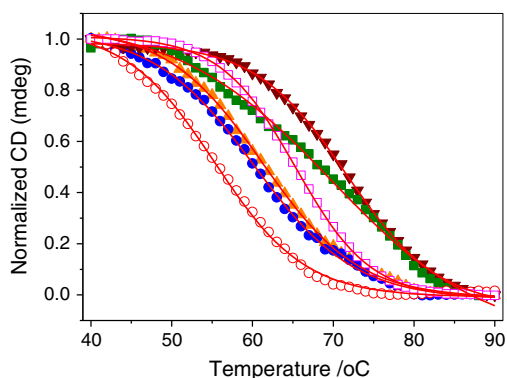


Fig. 2. Normalized CD melting curves for G-quadruplex DNA (○), G-quadruplex DNA + **1** (●), G-quadruplex DNA + **2** (▲) in Na^+ buffer (pH 7.0); G-quadruplex DNA (□), G-quadruplex DNA + **1** (■), G-quadruplex DNA + **2** (▼) in K^+ buffer (pH 7.0). [DNA] = 5 μM , [complex] = 5 μM . The stability of G-quadruplexes DNA was assessed by CD at 295 nm.

addition of 22AG to a solution of **2** in K^+ buffer led to a 22 nm red shift and 28.9% hypochromism of the band at 392 nm; however addition of 22 AG to the Na^+ buffered solution led to a 20 nm red shift and 23.7% hypochromism. The similar case could be seen for complex **1**, too. Hypochromism and red shift indicated strong interactions between the DNA bases and the complexes. Here the representative electronic spectral traces of both complexes titrated with 22AG in K^+ buffered solutions were given in Fig. 3. The others and related quantitative data were shown in Table 1.

In order to compare quantitatively the binding strength of $[\text{Ru}(\text{phen})_2(\text{L})]^{2+}$ to each G-quadruplexes DNA, the intrinsic binding constants K with each DNA at 25 $^{\circ}\text{C}$ were obtained using the following Eqs. (2a) and (2b) [61–63],

$$(\varepsilon_a - \varepsilon_f) / (\varepsilon_b - \varepsilon_f) = \left(b - (b^2 - 2K^2 C_t [\text{DNA}] / s)^{1/2} \right) / 2K C_t \quad (2a)$$

$$b = 1 + K C_t + K [\text{DNA}] / 2s \quad (2b)$$

where [DNA] is the concentration of DNA in base pair, ε_a , ε_f and ε_b are, the apparent extinction coefficient ($A_{\text{abs}}/[\text{M}]$), the extinction coefficient for free metal (M) complex and the extinction coefficient for the metal (M) complex in the fully bound form, respectively. K is the equilibrium binding constant in M^{-1} , C_t is the total metal complex concentration, and s is the binding size. As shown in Table 1, both complexes bind the mixed-hybrid quadruplex more avidly than that of antiparallel basket quadruplex DNA and complex **2** bind to the G-quadruplexes DNA more tightly than complex **1** does. The results obtained by absorption spectra titrations are overall consistent with those obtained by CD melting profiles.

To find out the stoichiometry interactions between complex and G-quadruplex DNA, we used the method of continuous variation known as Job plot. The results are displayed in Fig. 4. It is evident that the binding is determined to be 1:1. This binding stoichiometry suggests both complexes are interacting with each molecule of G-quadruplex DNA.

For both complexes **1** and **2**, no emission was observed either in Tris buffer or in the presence of G-quadruplexes DNA. To further clarify the nature of the interaction between the complex and DNA, G-quadruplex FID was carried out. FID is a simple and fast method to evaluate the affinity of a compound for G-quadruplex DNA [64–67]. This assay is based on the loss of fluorescence of thiazole orange (TO) upon competitive displacement from DNA by a putative ligand. Upon interaction with quadruplex DNA, TO exhibits high affinity ($K = 3 \times 10^6 \text{ M}^{-1}$) and displays a significant increase in its fluorescence, whereas when free in solution, the fluorescence is quenched. Therefore, the affinity of a molecule for quadruplex DNA is estimated by the DC_{50} value, which corresponds to the required concentration of complex to induce a 50% fluorescence decrease. The fluorescence area (FA, 500–750 nm), converted in percentage displacement (PD, with $\text{PD} = 100 - [(FA/FA_0) \times 100]$, FA_0 being FA before addition of complex), is then plotted versus the concentration of added complex.

We were first interested in comparing the quadruplex DNA binding abilities of the free ligands and the corresponding metal complexes. The emission spectra of TO bound to DNA in the absence and the presence of complex or ligand are shown in Fig. 5. We can see that the addition of either complex **1** or complex **2** to DNA pretreated TO causes appreciable reduction in the emission intensity (Fig. 5(a), (b)). The DC_{50} values are summarized in Table 2. Several interesting trends emerge from these studies: both complexes displace TO at low μM concentrations suggesting strong interactions between these complexes and telomeric quadruplex DNA, which are comparable to those found for other compounds reported to be good quadruplex DNA binders [67–69]. In contrast, no obvious displacement was observed induced by bppp. Similarly, pppp is not able to fully displace TO, even at concentrations as

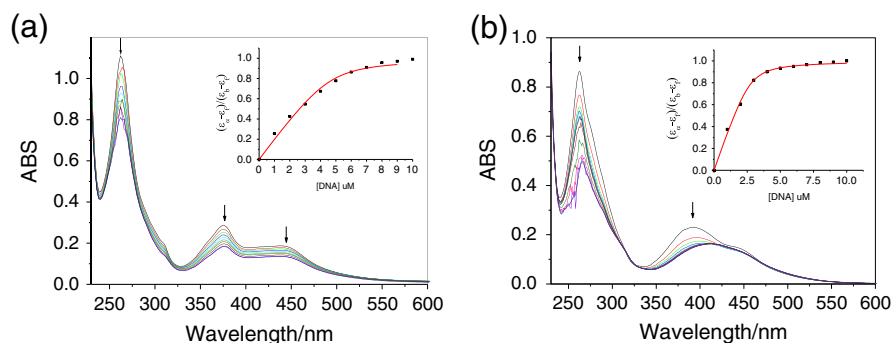


Fig. 3. Absorption spectra of complex **1** (a) and complex **2** (b) in K^+ buffered solutions in the presence of 22AG ([complex] = $10 \mu\text{M}$, [DNA] = $0\text{--}10 \mu\text{M}$). Arrow shows the absorbance change upon increasing DNA concentration. Inset: plot of $(\epsilon_a - \epsilon_f)/(\epsilon_b - \epsilon_f)$ vs. [DNA] for the titration of Ru(II) complexes.

high at $10 \mu\text{M}$ and only 5–10% displacement at $2.5 \mu\text{M}$. The results indicate that the free ligands do not display significant intermolecular $\pi\text{--}\pi$ stacking interaction while the corresponding complexes do. Another important observation from the data shown in Table 2 is that DC_{50} values in K^+ buffer (for the mixed-hybrid quadruplex) are smaller than those of Na^+ buffer (antiparallel basket quadruplex). However, no marked buffer effect was observed in absorption spectra studies. This difference might be caused by the different spectroscopy method. Compared with absorption spectra studies, FID assay is more sensitive to buffers and DNA structures. So buffer effect was observed from FID data.

The selectivity of both complexes for quadruplex DNA versus duplex DNA was then carried out. Though both complexes showed prominent G-quadruplex binding affinity, a modest selectivity for quadruplex over duplex was observed (Table 2). It is also worth pointing out that, although the differences are small, complex **2** was found to have a stronger preference for binding to the mixed-hybrid G-quadruplex over duplex DNA (binding up to 3 times better to the mixed-hybrid quadruplex DNA than to duplex DNA). This indicated that modifying the complex could create some interesting differences in the DNA-binding properties, therefore, such structural information of the complexes was still important for a more comprehensive understanding of the biological implications of these structures and for designing new drugs with enhanced activity and minimized undesired toxicity.

To gain insight into interaction between complex and G-quadruplex, molecular docking studies were carried out, which could corroborate the experimental results [49,70,71]. The antiparallel basket NMR G-quadruplex structure (PDB ID: 143D) and a 26-mer mixed-hybrid type G-quadruplex structure (PDB ID: 2HY9) were used as the templates for the docking studies. To compare both conformations, we removed two adenines from each end of the mixed-hybrid structure. As shown in Fig. 6, the docking study confirms that each intramolecular

G-quadruplex molecule binds to one $[\text{Ru}(\text{phen})_2(\text{L})]^{2+}$ molecule. It has been previously shown that G-quadruplex binders can stack on the surface of both terminal G-quartet planes. Complexes **1** and **2** contain a square π -aromatic surface, both bppp and pppp preferred to stack in the center of a terminal G-quartet end. For antiparallel basket G-quadruplex structure, both diagonal loop and parallel loop binding positions were considered. When $[\text{Ru}(\text{phen})_2(\text{L})]^{2+}$ binds in the diagonal loop position, $\pi\text{--}\pi$ stacking become less stable than in the parallel loop binding position as showed energy calculation results. So both complexes prefer to stack on the center of between the parallel loop and terminal G-quartet (Fig. 6(a), (c)). As for the mixed-hybrid G-quadruplex DNA, the predicted most favorable binding site between $[\text{Ru}(\text{phen})_2(\text{L})]^{2+}$ and G-quadruplex DNA was stacking on the external G-quartets at the 5' end of oligonucleotide (Fig. 6(b), (d)). A higher planar area, an extended π system, hydrophobicity, and aromaticity of complex **2** lead to better stacking within the base-pairs of DNA than complex **1** does. This proposed model is supported by molecular modeling study of the binding interactions between complex and G-quadruplex DNA. The favorable calculated binding free energies of complex **1** with G-quadruplex DNA are -11.2 and -9.3 kcal/mol for the mixed-hybrid G-quadruplex and the antiparallel basket G-quadruplex, respectively. The favorable calculated binding free energies of complex **2** with G-quadruplex DNA are -12.2 and -10.1 kcal/mol for the mixed-hybrid G-quadruplex and the antiparallel basket G-quadruplex, respectively. The lower binding free energy of complex **2** also suggests more favorable binding interactions with G-quadruplexes DNA than complex **1**. It was also noteworthy that both complexes possessed

Table 1
Absorption spectra ($\lambda_{\text{max}}/\text{nm}$) and G-quadruplexes DNA-binding constants K_b ($\times 10^5 \text{M}^{-1}$) of **1** and **2** in different buffers.

Complex	$\lambda_{\text{max}}/\text{free}$	$\lambda_{\text{max}}/\text{bound}$	$\Delta\lambda/\text{nm}$	H (%) ^a	$K/10^5 \text{M}^{-1}$	s
1 (K^+)	262	263	1	22.6	3.8 ± 0.3	1.2
	376	376	0	35.9		
	438	438	0	27.8		
1 (Na^+)	262	262	0	22.0	3.3 ± 0.2	0.9
	376	376	0	27.1		
	438	438	0	18.4		
2 (K^+)	262	265	3	40.5	8.3 ± 0.5	1.4
	392	413	22	28.9		
	262	263	1	34.9		
2 (Na^+)	392	412	20	23.7	6.1 ± 0.2	1.3

^a H : hypochromism.

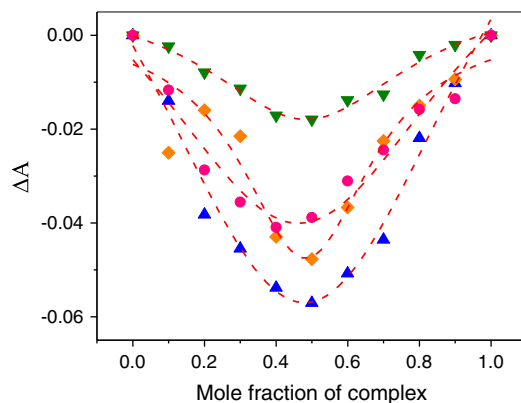


Fig. 4. Job's plots of complex **1** binding to 22AG in Na^+ (∇) and K^+ (\bullet) buffer; Job's plots of complex **2** binding to 22AG in Na^+ (\diamond) and K^+ (\blacktriangle) buffer. Total concentration (complex + DNA) = $10 \mu\text{M}$. ΔA is the calculated absorption difference at wavelengths 376 and 392 nm for complexes **1** and **2**, respectively.

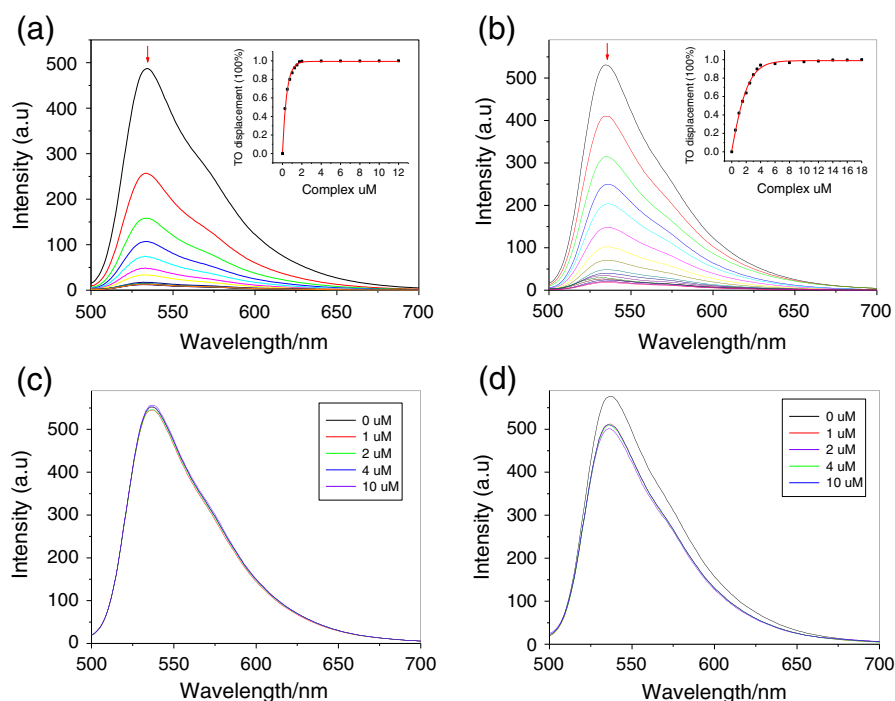


Fig. 5. Fluorescence displacement of TO bound G-quadruplex DNA by complex **1** (a), **2** (b), ligand bppp (c) and pppp (d) in K^+ buffer. Arrow shows the intensity changes upon increasing the concentration of complex **1** or complex **2**. Inset: FID results onto 22AG for complex **1** or complex **2**.

much more favorable binding interactions (lower binding free energy) with the mixed-hybrid G-quadruplex than antiparallel basket G-quadruplex. Such reliable end-stacking of compounds onto the G-quartet are in agreement with previous aromatic quadruplex binders [72]. Thus, molecular modeling studies explained the different binding affinities and confirmed the excellent complementarity in binding modes.

4. Conclusions

In summary, two new polypyridyl ligands (bppp and pppp), and their mixed-ligand ruthenium(II) complexes $[Ru(phen)_2(bppp)]^{2+}$ (**1**) and $[Ru(phen)_2(pppp)]^{2+}$ (**2**), have been synthesized and characterized. A comparison of the G-quadruplex DNA binding abilities of the free ligands and the corresponding metal complexes, has shown the important role played by the octahedral ruthenium(II) center in yielding good G-quadruplex DNA binders. The 1:1 stoichiometry suggests that both complexes are interacting with each molecule of G-quadruplex DNA. Furthermore, both complexes bind the mixed-hybrid G-quadruplex more avidly than that of antiparallel basket G-quadruplex DNA and complex **2** bind to the G-quadruplexes DNA more tightly than complex **1** does. However, the selectivity of the complexes for G-quadruplex versus duplex DNA is not as high as initially expected. Studies carried out so far have revealed that

modification of main ligand could create some interesting differences in the DNA-binding properties. Designing new complexes with enhanced activity and minimized undesired toxicity is currently being investigated in our laboratory.

Abbreviations

phen	1,10-phenanthroline
bppp	12-bromo-pyrido[2',3':5,6]pyrazino[2,3-f][1,10]phenanthroline
pppp	12-phenylpyrido[2',3':5,6]pyrazino[2,3-f][1,10]phenanthroline
dppz	dipyrido[3,2-a:2',3'-c]phenazine
Pd(PPh ₃) ₄	tetrakis(triphenylphosphine) palladium(0)
TO	Thiazole orange
22AG	5'-AGGGTTAGGGTTAGGGTTAGGG-3'
G-4	G-quadruplex
ds	Duplex strand
MLCT	Metal-to-ligand charge transfer
IL	Intraligand
ESI-MS	Electrospray ionisation mass spectra
FAB-MS	Fast atom bombardment mass spectra
UV-Vis	UV-visible
CD	Circular dichroism
FID	Fluorescent intercalator displacement
PDB	Protein Data Bank
DFT	Density Functional Theory
PDBQT	Protein Data Bank, Partial Charge (Q), & Atom Type (T)

Table 2

$G^{-4}DC_{50}$ and $dsDC_{50}$ values (μM) determined using FID assay for complexes **1** and **2**^a.

Complex	TO displacement		Selectivity
	$G^{-4}DC_{50}$ (μM)	$dsDC_{50}$ (μM)	
1 (K^+)	0.96 ± 0.15	1.45 ± 0.21	1.5
1 (Na^+)	1.55 ± 0.24	1.96 ± 0.22	1.3
2 (K^+)	0.42 ± 0.10	1.34 ± 0.17	3.2
2 (Na^+)	1.46 ± 0.19	1.64 ± 0.13	1.1

^a Values are average of three independent measurements.

Acknowledgments

This work was supported by the National Natural Science Foundation of China (20901060, 31170776, 81171646) and the Fundamental Research Funds for the Central Universities.

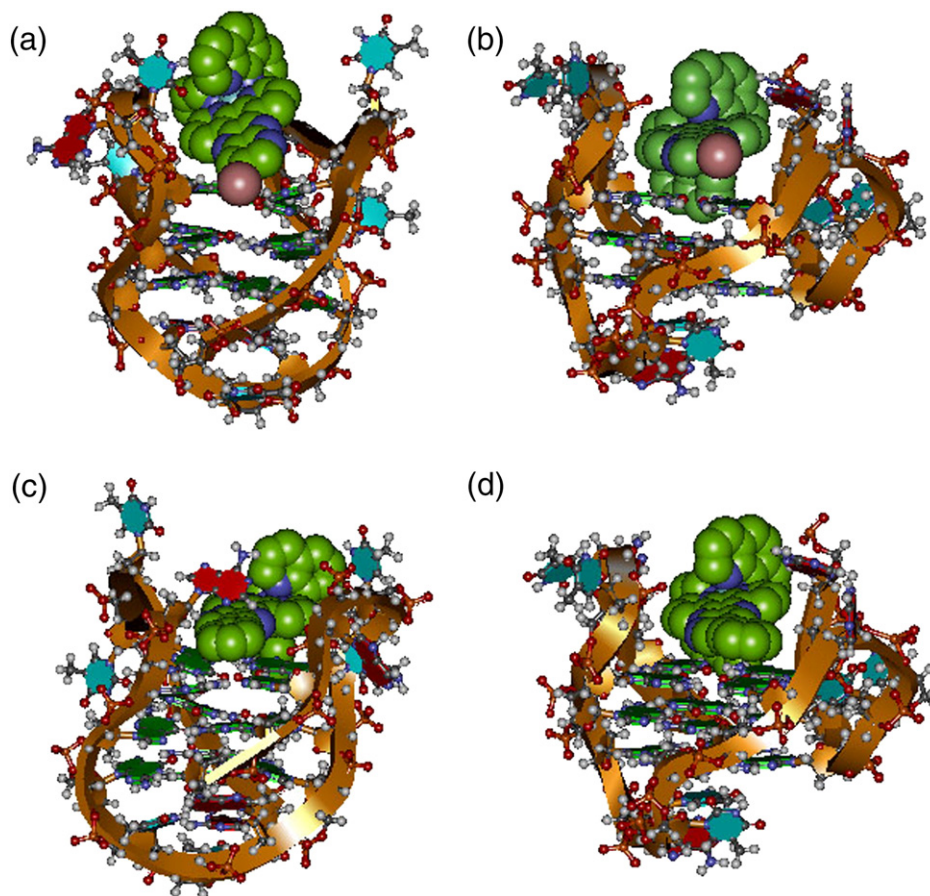


Fig. 6. Schematic diagram of the interaction of complex 1 with the antiparallel G-quadruplex structure (a) and the mixed-hybrid G-quadruplex structure (b); schematic diagram of the interaction of complex 2 with the antiparallel G-quadruplex structure (c) and the mixed-hybrid G-quadruplex structure (d). The G-quadruplexes and complexes are shown in ribbon and CPK mode, respectively.

Appendix A. Supplementary data

The spectra of NMR as well as their assignments (Fig. s1) are included in the supplementary material. Supplementary data associated with this article can be found, in the online version at <http://dx.doi.org/10.1016/j.jinorgbio.2012.12.011>.

References

- [1] M. Gellert, M.N. Lipsett, D.R. Davies, *Proc. Natl. Acad. Sci. U. S. A.* 48 (1962) 2013–2018.
- [2] S. Neidle, S. Balasubramanian, *Quadruplex Nucleic Acids*, Royal Society of Chemistry, Cambridge, 2006.
- [3] J.T. Davis, *Angew. Chem. Int. Ed.* 43 (2004) 668–698.
- [4] J.L. Huppert, *Biochimie* 90 (2008) 1140–1148.
- [5] A.K. Todd, M. Johnston, S. Neidle, *Nucleic Acids Res.* 33 (2005) 2901–2907.
- [6] K. Suntharalingam, A.J.P. White, R. Vilar, *Inorg. Chem.* 48 (2009) 9427–9435.
- [7] D. Yang, K. Okamoto, *Future Med. Chem.* 2 (2010) 619–646.
- [8] Y. Wang, D.J. Patel, *Structure* 1 (1993) 263–282.
- [9] G.N. Parkinson, M.P.H. Lee, S. Neidle, *Nature* 417 (2002) 876–880.
- [10] A. Ambrus, D. Chen, J.X. Dai, T. Bialis, R.A. Jones, D. Yang, *Nucleic Acids Res.* 34 (2006) 2723–2735.
- [11] Y. Xu, Y. Noguchi, H. Sugiyama, *Bioorg. Med. Chem.* 14 (2006) 5584–5591.
- [12] T.M. Ou, Y.J. Lu, J.H. Tan, Z.S. Huang, K.Y. Wong, L.Q. Gu, *ChemMedChem* 3 (2008) 690–713.
- [13] M. Wieland, J. Hartig, *Angew. Chem. Int. Ed.* 45 (2006) 5875–5878.
- [14] S. Neidle, G.N. Parkinson, *Curr. Opin. Struct. Biol.* 13 (2003) 275–283.
- [15] T.R. Cech, *Angew. Chem. Int. Ed.* 112 (2000) 34–43.
- [16] A. Siddiqui-Jain, C.L. Grand, D.J. Bearss, L.H. Hurley, *Proc. Natl. Acad. Sci. U. S. A.* 99 (2002) 11593–11598.
- [17] J. Dai, T.S. Dexheimer, D. Chen, M. Carver, A. Ambrus, R.A. Jones, D. Yang, *J. Am. Chem. Soc.* 128 (2006) 1096–1098.
- [18] S. Balasubramanian, L.H. Hurley, S. Neidle, *Nat. Rev. Drug Discov.* 10 (2011) 261–275.
- [19] L.K. White, W.E. Wright, J.W. Shay, *Trends Biotechnol.* 19 (2001) 114–120.
- [20] E.M. Rezler, D.J. Bearss, L.H. Hurley, *Curr. Opin. Pharmacol.* 2 (2002) 415–423.
- [21] H.J. Lipps, D. Rhodes, *Trends Cell Biol.* 19 (2009) 414–422.
- [22] A. Agrawal, S. Dang, R. Gabrani, *Recent Pat. Anticancer Drug Discov.* 7 (2012) 102–117.
- [23] M.A. Read, J.R. Harrison, B. Romagnoli, F.A. Tanious, S.H. Gowan, A.P. Reszka, W.D. Wilson, L.R. Kelland, S. Neidle, *Proc. Natl. Acad. Sci. U. S. A.* 98 (2001) 4844–4849.
- [24] I.M. Dixon, F. Lopez, J.P. Esteve, A.M. Tejera, M.A. Blasco, G. Pratviel, B. Meunier, *ChemBioChem* 6 (2005) 123–132.
- [25] F. Koeppel, J.F. Riou, A. Laoui, P. Mailliet, P.B. Arimondo, D. Labit, O. Petitgenet, C. Helene, J.L. Mergny, *Nucleic Acids Res.* 29 (2001) 1087–1096.
- [26] G.R. Clark, P.D. Pytel, C.J. Squire, S. Neidle, *J. Am. Chem. Soc.* 125 (2003) 4066–4067.
- [27] W. Tuntiwechapakul, J.T. Lee, M. Salazar, *J. Am. Chem. Soc.* 123 (2001) 5606–5607.
- [28] M.Y. Kim, H. Vankayalapati, K. Shin-ya, K. Wierzbica, L.H. Hurley, *J. Am. Chem. Soc.* 124 (2002) 2098–2099.
- [29] S.N. Georgiades, N.H.A. Karim, K. Suntharalingam, R. Vilar, *Angew. Chem. Int. Ed.* 49 (2010) 4020–4034.
- [30] Y.L. Jiang, Z.P. Liu, *Mini-Rev. Med. Chem.* 10 (2010) 726–736.
- [31] S. Shi, J. Liu, T.M. Yao, X.T. Geng, L.F. Jiang, Q.Y. Yang, L. Cheng, L.N. Ji, *Inorg. Chem.* 47 (2008) 2910–2912.
- [32] H. Bertrand, D. Monchaud, A.D. Cian, R. Guillot, J.L. Mergny, M.P. Teulade-Fichou, *Org. Biomol. Chem.* 5 (2007) 2555–2559.
- [33] H. Bertrand, S. Bombard, D. Monchaud, M.P. Teulade-Fichou, *J. Biol. Inorg. Chem.* 12 (2007) 1003–1014.
- [34] K.E. Erkila, D.T. Odom, J.K. Barton, *Chem. Rev.* 99 (1999) 2777–2796.
- [35] C. Metcalfe, J.A. Thomas, *Chem. Soc. Rev.* 32 (2003) 215–224.
- [36] S.P. Foxon, T. Phillips, M.R. Gill, M. Towrie, A.W. Parker, M. Webb, J.A. Thomas, *Angew. Chem. Int. Ed.* 46 (2007) 3686–3688.
- [37] J.K. Barton, E.D. Olmon, P.A. Sontz, *Coord. Chem. Rev.* 255 (2011) 619–634.
- [38] J.G. Genevieux, J.K. Barton, *Chem. Rev.* 110 (2010) 1642–1662.
- [39] S. Shi, J. Zhao, X.T. Geng, T.M. Yao, H.L. Huang, T.L. Liu, L.F. Zheng, Z.H. Li, D. Yang, L.N. Ji, *Dalton Trans.* 39 (2010) 2490–2493.
- [40] S. Shi, X.T. Geng, J. Zhao, T.M. Yao, C.R. Wang, D.J. Yang, L.F. Zheng, L.N. Ji, *Biochimie* 92 (2010) 370–377.
- [41] S. Shi, J. Zhao, X. Gao, L. Yang, J. Hao, C.Y. Lv, H.L. Huang, T.M. Yao, L.N. Ji, *Dalton Trans.* 41 (2012) 5789–5793.
- [42] M. Yamada, Y. Tanaka, Y. Yoshimato, S. Kuroda, I. Shimao, *Bull. Chem. Soc. Jpn.* 65 (1992) 1006–1011.

- [43] C.R. Cantor, M.M. Warshaw, H. Shapiro, *Biopolymers* 9 (1970) 1059–1077.
- [44] P.J. Hay, W.R. Wadt, *J. Chem. Phys.* 82 (1985) 270–283.
- [45] G.M. Morris, D.S. Goodsell, R. Huey, *User's guide AutoDock –automated docking of flexible ligands to receptors*, The Scripps Research Institute, Molecular Graphics Laboratory, 2001. (Available at: <http://autodock.scripps.edu/faqs-help/manual/autodock-3-user-s-guide>).
- [46] R. Huey, G.M. Morris, *Using AutoDock4 with AutoDockTools: A tutorial*, The Scripps Research Institute, Molecular Graphics Laboratory, La Jolla, CA, 2008.
- [47] T.N. Hasan, L. Grace B, T.A. Masoodi, G. Shafi, A.A. Alshatwi, P. Sivashanmugham, *Adv. Appl. Bioinform. Chem.* 4 (2011) 29–36.
- [48] S. Agrawal, R.P. Ojha, S. Maiti, *J. Phys. Chem. B.* 112 (2008) 6828–6836.
- [49] D. Sahoo, P. Bhattacharya, S. Chakravorti, *J. Phys. Chem. B.* 114 (2010) 2044–2050.
- [50] S. Haider, S. Neidle, *Meth. Mol. Biol.* 608 (2010) 17–37.
- [51] S. Thangapandian, S. John, S. Sakkiiah, K.W. Lee, *J. Chem. Inf. Model.* 51 (2011) 33–44.
- [52] C. Antonacci, J.B. Chaires, R.D. Sheardy, *Biochemistry* 46 (2007) 4654–4660.
- [53] S. Paramasivan, I. Rujan, P.H. Bolton, *Methods* 43 (2007) 324–331.
- [54] J.S. Hudson, S.C. Brooks, D.E. Graves, *Biochemistry* 48 (2009) 4440–4447.
- [55] J. Dai, C. Punchedhewa, A. Ambrus, D. Chen, R.A. Jones, D. Yang, *Nucleic Acids Res.* 35 (2007) 2440–2450.
- [56] J.L. Zhou, Y.J. Lu, T.M. Ou, J.M. Zhou, Z.S. Huang, X.F. Zhu, C.J. Du, X.Z. Bu, L. Ma, L.Q. Gu, Y.M. Li, A.S.C. Chan, *J. Med. Chem.* 48 (2005) 7315–7321.
- [57] X. Li, Y.H. Peng, J.S. Ren, X.G. Qu, *Proc. Natl. Acad. Sci. U. S. A.* 26 (2006) 19658–19663.
- [58] J.Z. Wu, B.H. Ye, L. Wang, L.N. Ji, J.Y. Zhou, R.H. Li, Z.Y. Zhou, *Dalton Trans.* 8 (1997) 1395–1401.
- [59] X.H. Zou, B.H. Ye, H. Li, J.G. Liu, Y. Xiong, L.N. Ji, *Dalton Trans.* 9 (1999) 1423–1428.
- [60] S. Shi, T.M. Yao, X.T. Geng, L.L. Jiang, J. Liu, Q.Y. Yang, L.N. Ji, *Chirality* 21 (2009) 276–283.
- [61] S.R. Smith, G.A. Neyhart, W.A. Kalsbeck, H.H. Thorp, *New J. Chem.* 18 (1994) 397–406.
- [62] R.B. Nair, E.S. Teng, S.L. Kirkland, C.J. Murphy, *Inorg. Chem.* 37 (1998) 139–141.
- [63] M.T. Carter, M. Rodriguez, A.J. Bard, *J. Am. Chem. Soc.* 111 (1989) 8901–8911.
- [64] D. Monchaud, C. Allain, M.P. Teulade-Fichou, *Bioorg. Med. Chem. Lett.* 16 (2006) 4842–4845.
- [65] P.L.T. Tran, E. Largy, F. Hamon, M.P. Teulade-Fichou, J.L. Mergny, *Biochimie* 93 (2011) 1288–1296.
- [66] N.M. Smith, G. Labrunie, B. Corry, P.L.T. Tran, M. Norret, M. Djavaheri-Mergny, C.L. Raston, J.L. Mergny, *Org. Biomol. Chem.* 9 (2011) 6154–6162.
- [67] K. Suntharalingam, A.J.P. White, R. Vilar, *Inorg. Chem.* 49 (2010) 8371–8380.
- [68] D. Monchaud, C. Allain, H. Bertrand, N. Smargiasso, F. Rosu, V. Gabelica, A.D. Cian, J.L. Mergny, M.P. Teulade-Fichou, *Biochimie* 90 (2008) 1207–1223.
- [69] A. Arola-Arnal, J. Benet-Buchholz, S. Neidle, R. Vilar, *Inorg. Chem.* 47 (2008) 11910–11919.
- [70] S. Sparapani, S. Bellini, M. Gunaratnam, S.M. Haider, A. Andreani, M. Rambaldi, A. Locatelli, R. Morigi, M. Granaiola, L. Varoli, S. Burnelli, A. Leonib, S. Neidle, *Chem. Commun.* 46 (2010) 5680–5682.
- [71] S. Sparapani, S.M. Haider, F. Doria, M. Gunaratnam, S. Neidle, *J. Am. Chem. Soc.* 132 (2010) 12263–12272.
- [72] R. Kiełtyka, P. Englebienne, J. Fakhoury, C. Autexier, N. Moitessier, H.F. Sleiman, *J. Am. Chem. Soc.* 130 (2008) 10040–10041.